



Low-symmetry A₃B type pentachlorocyclotriphosphazene substituted phthalocyanine with improved nonlinear optical properties: Synthesis, spectroscopic and *ab initio*/(TD)DFT study

Alexander Yu Tolbin^{a,*}, Valery K. Brel^b, Boris N. Tarasevich^c, Victor E. Pushkarev^{a,c}

^a Institute of Physiologically Active Compounds (IPAC RAS), Russian Academy of Sciences, 142432, Chernogolovka, Moscow Region, Russian Federation

^b A. N. Nesmeyanov Institute of Organoelement Compounds (INEOS RAS), Russian Academy of Sciences, 119991, Moscow Region, Russian Federation

^c Department of Chemistry M. V. Lomonosov Moscow State University, 119991, Moscow Region, Russian Federation

ABSTRACT

In the present work, we performed structural modification of 2-hydroxy-9(10),16(17),23(24)-tri-*tert*-butyl-29*H*,31*H*-phthalocyanine (**1**) using phosphonitrilic chloride trimer (hexachlorocyclotriphosphazene). Despite the wide availability of phosphazenes and their derivatives, including polymeric materials based on them, this is one of the few examples of the introduction of an active phosphazene cycle into the structure of a macroheterocyclic compound. Target free-base ligand **2** was characterized by the MALDI-TOF/TOF mass spectrometry, as well as the ¹H, ³¹P NMR and FT-IR spectroscopy. Also, a tendency towards *H*-aggregation in polar media was demonstrated. Theoretical calculations based on time-dependent Hartree-Fock approach for nonlinear optical properties have allowed revealing a self-defocusing effect in the case of phthalocyanine **2**, which makes it an interesting candidate for all-optical switching, two-photon imaging, and optical power limiting applications.

1. Introduction

Phthalocyanines are the macroheterocyclic organic dyes with an extended 18- π electron system and a flat structure [1,2]. Many essential applied properties of phthalocyanines are associated with their structural uniqueness, which results in intense absorption in the visible and near-IR regions, magnetic and semiconducting properties, as well as the nonlinear optical (NLO) response [3]. An important feature of phthalocyanines is that all their properties can be precisely tuned by simple chemical modifications. In this way, it is possible to achieve the required catalytic, sensory and photodynamic characteristics [2]. Lowering the symmetry of phthalocyanines, on the one hand, leads to a significant increase in the molecular polarizability under the external electric and/or magnetic fields, and introduction of the appropriate functional groups, on the other hand, allows the creation of the advanced nanoscale ensembles and composite materials [4,5]. Our recent works are related to the selective synthesis of the cofacial phthalocyanine dimers of *H*- and *J*-types [6–8]. We have shown that the introduction of phosphorus (V) fragments to the periphery of phthalocyanines noticeably affects their spectral and nano aggregation properties [9,10].

In this work, we modified 2-position of 2-hydroxy-9(10),16(17),23(24)-tri-*tert*-butyl-29*H*,31*H*-phthalocyanine with one cyclotriphosphazene fragment containing five highly mobile chlorine atoms.

This simple nucleophilic reaction has been carried out under very mild conditions and will further allow obtaining polynuclear ensembles with controlled aggregation and optical characteristics. A huge amount of evidence of the relevance of phosphazenes and their polymers was obtained over many years [11,12]. In particular, phosphazene-modified silica gels containing adsorbed particles of polyoxometalates can be used as promising catalysts for the desulfurization of diesel fuel [13]. Besides, advanced elastomers, anticancer agents, hydraulic fluids and lubricants, as well as the electrically conductive materials can be obtained. Binding of phthalocyanines and related macroheterocyclic compounds with phosphazenes is currently rare, moreover, there were no reactive groups in the obtained compounds [14–17]. Therefore, further chemical reactions became virtually impossible. Herein, we first show the fundamental possibility of selective obtaining the low-symmetric monophthalocyanine bearing a cyclotriphosphazene fragment with five active chlorine atoms, which can be further used for the synthesis of polymacrocyclic derivatives and nanomaterials with given aggregation, electrical and NLO characteristics.

* Corresponding author.

E-mail address: tolbin@ipac.ac.ru (A.Y. Tolbin).

<https://doi.org/10.1016/j.dyepig.2019.108095>

Received 30 August 2019; Received in revised form 18 November 2019; Accepted 30 November 2019

Available online 3 December 2019

0143-7208/© 2019 Elsevier Ltd. All rights reserved.

2. Experimental

2.1. General methods

All solvents were reagent-grade quality and were obtained directly from Aldrich. Phthalocyanine ligand **1** was synthesized according to our previously published procedure [18].

UV–Vis spectra were recorded on a Hitachi U-2900 spectrophotometer in a range of 250–1000 nm in CCl₄, acetone, and methanol. FT-IR spectrum of phthalocyanine **2** was obtained in ZnSe pellets on a Nicolet Nexus IR-Furje spectrometer. ¹H and ³¹P NMR spectra were recorded on a Bruker Avance III 500 MHz spectrometer. MALDI-TOF/TOF measurements were performed with a Bruker ULTRAFLEX II TOF/TOF spectrometer using 2,5-dihydroxybenzoic acid (DHB, Aldrich) as a matrix.

2.2. Quantum-chemical calculations

Quantum chemical calculations were performed using the GAMESS (US) software package [19] and 6–311++G** basis set. Primarily, the model structures related to phthalocyanines **1** and **2** were optimized on the B3LYP level of the density functional theory (DFT). The vibrational analysis was performed to confirm whether the optimized geometries correspond to local minima without imaginary frequencies. *Tert*-butyl substituents were replaced with hydrogen atoms to reduce calculation time. TD-B3LYP calculations were performed for analysis of the electronic transitions (S₀→S₁) to search for the charge transfer (CT) transitions. Further, *ab initio* calculations of the static and frequency-dependent (0.043 a.u.) polarizability (α), first (β) and second (γ) hyperpolarizabilities of model phthalocyanine ligands **1** and **2** were carried out within the framework of the time-dependent Hartree–Fock method (TDHF) to evaluate the ability of the model compounds to exhibit NLO properties. All the quantum chemical calculations (gas-phase) were performed on an Intel/Linux cluster (Joint Supercomputer Center of Russian Academy of Sciences – <http://www.jssc.ru>). Visualization of the optimized structures was performed with the Mercury program obtained from the Cambridge Crystallographic Data Centre (<http://www.ccdc.cam.ac.uk>). Visualization of the electronic density was accomplished with the IQmol program (<http://iqmol.org>). Structural parameters (distances and angles) were calculated with the Geometry Analyzer Module for EasyQuanto [20].

2.3. Synthesis

1,1,3,3,5-pentachloro-5-(2-oxy-9(10),16(17),23(24)-tri-*tert*-butyl-29H,31H-phthalocyaninato)-cyclotriphosphazene(2). To a solution of low-symmetry ligand **1** (200 mg, 0.28 mmol) in THF (30 mL) sodium hydride (20 mg, 0.83 mmol) was added, and the reaction mixture was further kept under reflux for 20 min. Next, an excess of phosphonitrilic chloride trimer (300 mg, 0.88 mmol) was added, and the boiling was continued for 10 min. After the reaction was finished (TLC control), the solvent was evaporated *in vacuo* followed by washing of the residue with the mixture of methanol/water (1:1) and chromatographic purification on Bio-Beads SX-1 (BIORAD®) with THF as the eluent to remove high molecular weight by-products. Target compound **2** was obtained in 81% yield (235 mg). MALDI-TOF/TOF (matrix – DHB): *m/z* 1009.1136 [M+2H]⁺, calcd for [C₄₄H₄₃Cl₅N₁₁OP₃] 1009.1308. ¹H NMR (MeONa-*d*₃/DMSO-*d*₆, δ/ppm): 9.11–9.24 (group m, 8H, α-H^{Ar}), 8.06–8.10 (group m, 4H, β-H^{Ar}), 1.72 (br s, 27H, H^{Tbu}). {¹H} ³¹P NMR (NEt₃/CDCl₃, δ_p/ppm): 22.45 (d, 2P, PCl₂, A₂), 12.60 (t, 1P, PCl(OPc), X), ²J_{P,P} = 59.6 Hz. UV–Vis (solvent), λ_{max}/nm (log ε): data for CCl₄: 337 (4.88), 660 (4.95), 695 (4.94); data for acetone: 341 (4.91), 607 (4.67), 658 (5.01), 689 (4.95); data for methanol: 328 (4.91), 607 (4.77), 654 (4.67), 690 (4.51). FT–IR (ZnSe): 3290 (NH), 2950–2860 (C_{Ar}–H), 1610 (C=N), 1200 (P=N), 1090 (P–O), 984 (P–O–C_{Ar}).

All the spectra the reader can find in the Electronic Supporting

Information.

3. Results and discussion

3.1. Synthesis and characterization

Interaction of asymmetrically substituted phthalocyanine **1** with hexachlorocyclotriphosphazene has produced the target compound **2** (Scheme 1). The reaction proceeds actively and is highly susceptible to the external side processes, as a result of which dimers, trimers, and polymers can be formed with the participation of the phosphazene cycle.

Also one cannot exclude oxidative processes and hydrolysis. For this reason, the reactions were carried out in an inert atmosphere (reaction mixtures were carefully deoxygenated), and THF or benzene which are used as solvents were subjected to additional drying. For the selective synthesis of product **2**, a threefold excess of hexachlorotriphosphazene is necessary. With a decrease in its quantity or temperature, the reaction selectivity drops, which is associated with the predominant formation of dimers and trimers. Alteration of the reaction conditions (Scheme 1) did not lead to an increase in the yield of phthalocyanine **2**. Thus, in anhydrous DMSO, gradual destruction of the phosphazene cycle in the presence of K₂CO₃, KOH or NaH as a base was observed. Increasing the reaction temperature accelerates destructive processes. It has been found that almost any highly polar solvent – sulfolane, DMF, HMPT, etc. – leads to the phosphazene cycle to be decomposed to a certain extent under the reaction conditions. Selectivity is improved by lowering the medium polarity. Thus, in absolute benzene, the yield of phthalocyanine **2** increases by up to 86%. The high chemical activity of chlorine atoms in product **2** limits the options for its isolation from the reaction mixture. In particular, it is impossible to use silica gel or aluminas, which are prone to covalent binding to the target product. We found that an optimal system for purification of **2** is based on the cross-linked polymer Bio-Beads SX-1 and absolute THF as the eluent. This allowed us to get rid of all by-products as efficiently as possible, and to isolate compound **2** in an individual pure form.

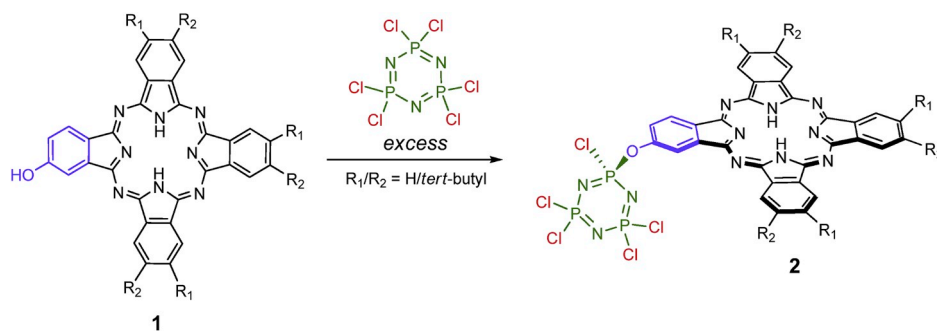
The MALDI-TOF/TOF mass spectrum of phthalocyanine **2** in the presence of DHB as the matrix demonstrates only the peak of molecular ion [M+2H]⁺ with clear isotopic pattern (Fig. S1). Minor fragmentation begins to occur without a matrix, which is associated with more severe ionization. In this case, [M–nCl]ⁿ⁺ (n = 1–3) and [M–Cl₄N₂P₂]²⁺ are observed as the essential ions.

The FT–IR spectrum of **2** confirms the embedding of the phosphazene fragment in the phthalocyanine periphery (Fig. S2), which follows from the appearance of an intense band at 1200 cm^{–1} (P=N bonds). Additional bands appear at 1090 and 984 cm^{–1} confirming the formation of the P–O–C bond.

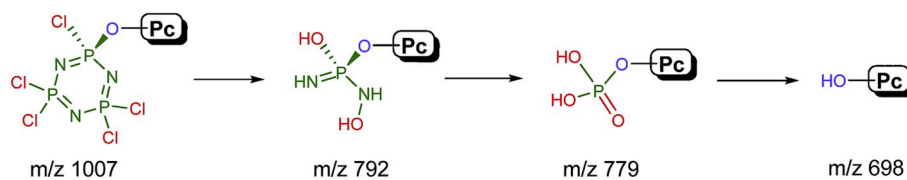
Target product **2** contains five mobile chlorine atoms in the phosphazene moiety, which can be used for further nucleophilic reactions to obtain heteroligand derivatives, as well as nanomaterials with covalent binding to the surface of nanotubes, graphene, etc. The phosphazene cycle can be considered as relatively stable. Only under very hard conditions, for example, in concentrated sulfuric acid, it is completely hydrolyzed to phosphoric acid, according to the MALDI-TOF mass spectrometry data. Thus, ion peaks with *m/z* 792 and 779 indicate consistent cleavage of the phosphazene cycle to *N*-hydroxyphosphoramidimide and phosphoric acids, respectively (Scheme 2):

Complete cleavage of the phosphazene cycle leads to the starting ligand **1** with substantial destruction of the phthalocyanine core due to the action of the phosphoric acid derivatives formed; meanwhile, starting compound **1** is stable in sulfuric acid both in solutions and after pouring onto the ice.

Thus, the revealed selective reaction conditions may further allow obtaining various derivatives with high yields, which will make them available for solving a lot of actual synthetic and practical problems.



Scheme 1. Selective synthesis of phosphazene-containing A₃B type phthalocyanine **2**. Reagents and conditions: NaH/THF, 60 °C, 30 min (81% yield), or NaH/benzene, 80 °C, 15 min (86% yield). [This is two-column image].



Scheme 2. Hydrolysis of phosphazene substituent in phthalocyanine **2** under the action of sulfuric acid, according to the MALDI-TOF/TOF analysis (see Fig. S3). [This is two-column image].

3.2. ¹H and ³¹P NMR spectroscopy

Newly synthesized phosphazene-containing phthalocyanine **2** shows aggregation tendency in such classical NMR solvents as CDCl₃ and DMSO-*d*₆ resulting in considerable widening of signals in ¹H and ³¹P spectra (Figs. S4 and S5). Thus, the proton decoupled ³¹P spectrum of **2** registered in pure CDCl₃ (Fig. S4) shows the weak unresolved signal of PCl(OPc) nuclei, while the PCl₂ signals demonstrate better resolution. Upon addition of NEt₃ to CDCl₃ solution, resolution of the ³¹P spectrum improves, and distinct signals can be observed (Fig. S6). Since the cyclotriphosphazene moiety of **2** represents A₂X spin system, the ³¹P NMR spectrum (Fig. S6) reveals a signal of two PCl₂ nuclei as a low-field doublet at 22.45 ppm and a signal of one PCl(OPc) nucleus as a higher-field triplet at 12.60 ppm. The ¹H NMR spectrum of **2** upon addition of NEt₃ to CDCl₃ also becomes more resolved, however not enough for careful assessment of purity and reliable assignment of the proton signals. To reach a good quality of the ¹H spectrum, we tried to carry out deprotonation of the Pc ligand in **2** with obtaining its dianionic species in conditions of the NMR experiment.

Recently, a disaggregating system represented as the solution of MeONa-*d*₃ in methanol-*d*₄ was developed in our group to obtain the resolved ¹H NMR spectra of a hydroxy-substituted phthalocyanine ligand and its aluminum complexes [21]. Due to poor solubility of **2** in this system, we modified it herein by replacing methanol-*d*₄ with DMSO-*d*₆. The resulting spectrum of deprotonated **2** (Fig. S5) reveals clear signals of α- and β-type protons in 9 and 8 ppm regions, respectively. Comparative analysis of ¹H, ³¹P NMR and UV-Vis spectra (Figs. S4–S7) evidence that π-π stacking interactions in **2** can be effectively damped only upon deprotonation of the Pc ligand. The addition of NEt₃ to CDCl₃ (CHCl₃) leads to only partial disaggregation implying that NEt₃ weakly affects the π-stacking and preferably solvates the phosphazene moiety.

3.3. UV-Vis spectroscopic study

The UV-Vis spectra of phthalocyanines **1** and **2** are shown in Fig. 1. They are typical for phthalocyanine ligands, where the Soret (B) and Q (Q_x, Q_y) bands are present, resulting from π → π* electronic transitions. According to the well-known concepts of phthalocyanine absorption spectroscopy, lowering the effective symmetry on the transition from

the metal complexes to the free-base ligands from D_{4h} or C_{4v} to D_{2h}, respectively, leads to the removal of the e_g LUMO degeneracy with the following splitting of e_g into b_{2g} and b_{3g} molecular orbitals of different energies [22–25]. This results in the splitting of the main absorption maxima, which is most evident in the Q-band case: two distinct components, Q_x and Q_y, are observed in the corresponding UV-Vis spectra (Fig. 1).

For phthalocyanines **1** and **2**, in the region of the electron-vibrational satellite (550–650 nm) some differences were found (Fig. 1a). Thus, the phosphazene-substituted ligand **2** reveals more intense vibrational bands than **1**, with them being observed in a narrower wavelength range. According to TD-B3LYP theoretical assessment, this is due to the overlay of an additional electronic transition, corresponding to the transfer of electron density from the macrocyclic contour to the phosphazene moiety: HOMO → LUMO+2 (Fig. 2).

This result might be the reason for the difference in spectral properties of phthalocyanines **1** and **2**. Thus, with increasing the solvent polarity, specific aggregation of both ligands is observed, with the phosphazene-substituted derivative **2** demonstrating a more significant enhancement of the aggregation processes. The UV-Vis absorption spectrum of starting ligand **1** in acetone (Fig. 1b) compared to the one in CCl₄ shows only slight changes, e.g. the blue shift of the Q_x component by 4 nm. At the same time, dye **2** in acetone begins to show a tendency toward *H*-aggregation, as seen from the appearance of the *H*-band in 600 nm region, as well as from a change in the intensity ratio of Q_x and Q_y components (Fig. 1b). In methanol, ligand **1** appears to initially form *H*-type dimers (Fig. 1c), since its absorption spectrum becomes similar to *clamshell*-type binuclear phthalocyanines, in which macrocycles are bound by a covalent spacer [26]. In the case of product **2**, the *H*-band in methanol has a higher intensity compared to the Q-band, and its significant broadening indicates the formation of *H*-aggregates. It is important to note that for both ligands **1** and **2**, the *H*-band appears near 600 nm and its position does not depend on the solvent nature, which indicates the similarity of these aggregation processes. The most efficient way to disassemble of *H*-aggregates is the deprotonation of the intracyclic phthalocyanine NH-groups. Thus, upon the addition of Et₃N to ligand **2**, minor changes begin to appear in the UV-Vis spectrum, which can be considered insignificant even after prolonged boiling. In turn, when phthalocyanine **2** interacts with MeOLi in methanol with stirring, the UV-Vis absorption shows a stepwise appearance of the

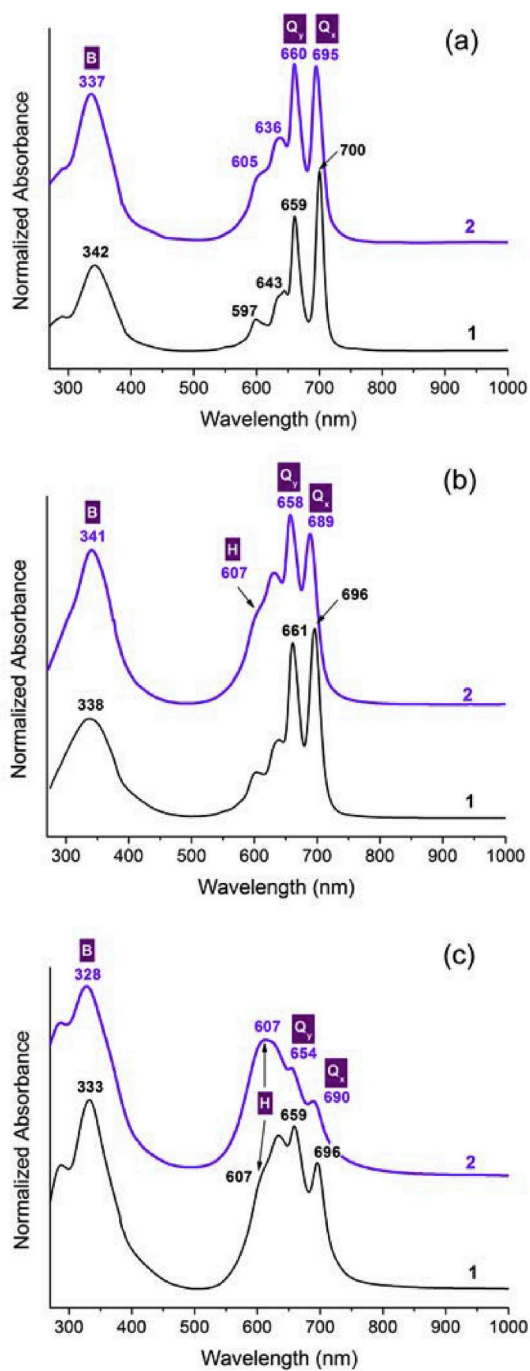


Fig. 1. UV-Vis absorption spectra ($C \approx 6 \times 10^{-6}$ M) of phthalocyanines 1 and 2 in different solvents: (a) CCl_4 , (b) acetone, (c) methanol. [This is one-column image].

dianionic form with the Q-band at 672 nm (Fig. S7), while the H-aggregate bands at 328 and 607 nm gradually decrease their intensity. It is important to note that reverse protonation of 2 with aqueous acetic acid promotes back the formation of H-aggregates, since the UV-Vis absorption spectrum returns to its original shape.

Also worth noting is the fact that phosphazene-substituted ligand 2 exhibits a blue shift of the Q-band components, compared with the precursor 1. This fact is due to the increase in the width of the bandgap by $\Delta E_g = 0.045$ eV (Table 1). It also follows from the calculations that the presence of cyclotriphosphazene substituents in the phthalocyanine molecule should lead to a significant increase in the basicity of the macrocyclic system.

3.4. NLO properties

To calculate the linear and nonlinear optical properties for closed-shell molecules one can apply *ab initio* time-dependent Hartree-Fock (TDHF) approach for NLO properties, which operates with sum-over-states (SOS) formalism to determine the optical response [27]. This method permits the analytic calculation of various static and/or frequency-dependent (hyper)polarizabilities to predict second and third-order NLO properties, such as second harmonic generation (SHG), electro-optic Pockels effect (EOPE), optical rectification (OR), third-harmonic generation (THG), electric-field induced second harmonic generation (EFISH), intensity-dependent refractive index (IDRI), optical Kerr effect (OKE), etc [28].

The structures of compounds 1 and 2 have been optimized on the RHF/6-311++G** level of theory (Fig. S8). Peripheral modification of ligand 1 leads to an increase in the C-O bond length by 0.042 Å. At the same time, the P-Cl bond length and the Cl-P-Cl bond angle are the same as in the original phosphazene. The dihedral angle between the planes of the phosphazene and phthalocyanine cycle is 16 deg., and the mutual rotation of these cycles is not energetically favorable. This result explains the specificity of the aggregation processes that we observed during the study of phthalocyanines 1 and 2 by the UV-Vis spectroscopy.

Simulation results obtained with the TDHF approach showed that the introduction of even one phosphazene cycle into the phthalocyanine structure leads to an increase in dipole moment $\Delta\mu$ by 1.298 D, which, of course, is favorable for the NLO properties. The isotropic dipole polarizability α , the magnitude of total first β and second γ static/frequency depended (0.043 a.u.) hyperpolarizabilities have been calculated using the following expressions, respectively [29]:

$$\alpha = (\alpha_{xx} + \alpha_{yy} + \alpha_{zz})/3 \quad (1)$$

$$\beta = (\beta_x^2 + \beta_y^2 + \beta_z^2)^{1/2}, \quad (2)$$

Where

$$\beta_i (i = x, y, z) = (1/3) \sum_{j=x,y,z} (\beta_{ij} + \beta_{ji} + \beta_{ji}) \quad (3)$$

$$\gamma = (1/5) [\gamma_{xxxx} + \gamma_{yyyy} + \gamma_{zzzz} + 2(\gamma_{xyxy} + \gamma_{xxzz} + \gamma_{yyzz})] \quad (4)$$

The results are presented in Table 2.

Phosphazene-substituted phthalocyanine 2 demonstrates clear advantages over hydroxyphthalocyanine 1 concerning the vast majority of NLO applications. An increase in the structural asymmetry of 2 leads to an enhancement of the NLO response and, at the same time, to the appearance of an important feature, expressed in the fact that the second hyperpolarizability in all cases, except the THG effect, has a negative sign. Organic materials with the negative real part of the molecular third-order polarizability $\text{Re}(\gamma)$ are extremely rare and are promising for all-optical switching, two-photon imaging, and optical power limiting applications. These materials are self-defocusing. In contrast to product 2, hydroxyphthalocyanine 1 exhibits a self-focusing effect, and the enormous values of nonlinear susceptibility for this compound in the EOPE and OKE effects argue in favor of its promise as an optical switch.

4. Conclusion

In this work, we first prepared an A₃B-type low-symmetry phthalocyanine substituted with the cyclotriphosphazene moiety. Thus, we implemented the directed synthesis of monophthalocyanine 2, bearing a phosphazene cycle with five active chlorine atoms. These chlorine substituents can further be used to enrich the structure, as well as for the functionalization of nanomaterials. The phosphazene unit leads to a huge structural asymmetry of 2, unusual aggregation properties

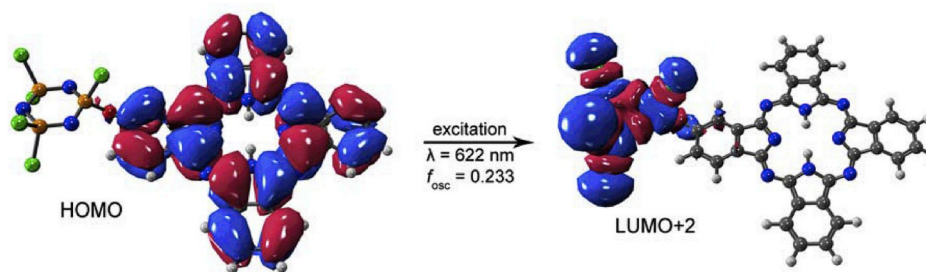


Fig. 2. Molecular orbitals which responsible for the total migration of electronic density on excitation in the vibrational satellite area of phosphazene-substituted phthalocyanine 2: TD-B3LYP calculations with visualization of the electron density. [This is two-column image].

Table 1

Selected calculation parameters of phthalocyanines 1 and 2 (B3LYP/6-311++G**).

Property	Compound 1 ^a	Compound 2 ^a
Dipole moment (μ), D	2.349	3.647
Bandgap (E_g) ^b , eV	1.382	1.427
The energy of orbitals (E), eV		
HOMO-1	1.24	-6.25
HOMO	1.48	-5.17
LUMO	2.86	-3.74
LUMO+1	2.88	-3.68

^a Calculations for Models A,B corresponded to compounds 1 and 2 (see Fig. S8).

^b $E_g = E_{\text{LUMO}} - E_{\text{HOMO}}$.

Table 2

NLO response for model compounds 1 and 2 based on TDHF calculation method.

Property	Compound 1 ^a	Compound 2 ^a
Static parameters ($F \rightarrow 0$ a.u. or $\lambda \rightarrow \infty$)		
Polarizability (α , \AA^3)	36.30	46.54
First hyperpolarizability ($\beta \times 10^{-29}$ esu)	1.31	1.83
Second hyperpolarizability ($\gamma \times 10^{-34}$ esu)	2.18	-2.15
Calculation for a frequency of $F = 0.043$ a.u. ($\lambda = 1.064 \mu$)		
Polarizability (α , \AA^3)	37.65	50.49
Second-order properties ($\beta \times 10^{-29}$ esu)		
Second-harmonic generation	-	26.04
Optical rectification	1.55	3.19
Electrooptic Pockels effect	1.36×10^2	3.20
Third-order properties ($\gamma \times 10^{-34}$ esu)		
Third harmonic generation	-	7.78
Electric-field induced the second harmonic generation	-	-33.17
Intensity-dependent refractive index	-	-6.43
Optical Kerr effect	4.95×10^3	-3.95

^bSee main text.

^a Calculations for Models A,B corresponded to compounds 1 and 2 (see Fig. S8).

expressed in the *H*-association of macrocycles, as well as the self-defocusing effect, according to TDHF calculations, which is important for a variety of NLO applications.

Author statement

Alexander Yu. Tolbin: Conceptualization, Methodology, Validation, Writing - Review & Editing.

Valery K. Brel: Resources.

Boris N. Tarasevich: Investigation.

Victor E. Pushkarev: Supervision, Funding acquisition.

Declaration of competing interest

No conflict of interest.

Acknowledgments

This work was generally supported by the Council under the President of the Russian Federation for State Support of Young Scientists and Leading Scientific Schools (Grant MD-3847.2019.3). We also acknowledge the support of spectral studies by the State Assignment of 2019 (Theme 45.5 Creation of compounds with given physicochemical properties, No 0090-2019-0003). The authors also thank the Joint Supercomputer Centre of RAS (www.jssc.ru) for providing computing resources.

Appendix A. Supplementary data

Supplementary data to this article can be found online at <https://doi.org/10.1016/j.dyepig.2019.108095>.

References

- [1] Arslan T, Çakır N, Keleş T, Biyiklioglu Z, Senturk M. Triazole substituted metal-free, metallo-phthalocyanines and their water soluble derivatives as potential cholinesterases inhibitors: design, synthesis and in vitro inhibition study. *Bioorg Chem* 2019;90:103100.
- [2] Mohammed I, Oluwale DO, Nemakal M, Sannegowda LK, Nyokong T. Investigation of novel substituted zinc and aluminium phthalocyanines for photodynamic therapy of epithelial breast cancer. *Dyes Pigments* 2019;170:107592.
- [3] Kabwe KP, Louzada M, Britton J, Olomola TO, Nyokong T, Khene S. Nonlinear optical properties of metal free and nickel binuclear phthalocyanines. *Dyes Pigments* 2019;168:347-56.
- [4] Yu Tolbin Alexander, Tomilova Larisa G, Zefirov NS. Non-symmetrically substituted phthalocyanines: synthesis and structure modification. *Russ Chem Rev* 2007;76(7):681.
- [5] Savelyev MS, Gerasimenko AY, Podgaetskii VM, Tereshchenko SA, Selishchev SV, Tolbin AY. Conjugates of thermally stable phthalocyanine J-type dimers with single-walled carbon nanotubes for enhanced optical limiting applications. *Opt Laser Technol* 2019;117:272-9.
- [6] Tolbin AY, Pushkarev VE, Balashova IO, Dzuban AV, Tarakanov PA, Trashin SA, Tomilova LG, Zefirov NS. A highly stable double-coordinated 2-hydroxy-tri(tert-butyl)-substituted zinc phthalocyanine dimer: synthesis, spectral study, thermal stability and electrochemical properties. *New J Chem* 2014;38(12):5825-31.
- [7] Tolbin AY, Pushkarev VE, Tomilova LG, Zefirov NS. Threshold concentration in the nonlinear absorbance law. *Phys Chem Chem Phys* 2017;19(20):12953-8.
- [8] Tolbin AY, Pushkarev VE, Tomilova LG, Zefirov NS. Monohydroxyphthalocyanines as potential precursors to create nanoscale optical materials. *J Porphyr Phthalocyanines* 2017;21(02):128-34.
- [9] Tolbin AY, Pushkarev VE, Balashova IO, Brel VK, Gudkova YI, Shestov VI, Tomilova LG. Synthesis of phthalocyanine compounds bearing 2-(diethoxyphosphoryl)-4-methylpenta-1,3-dienyl functional groups. *J Porphyr Phthalocyanines* 2013;17(05):343-50.
- [10] Tolbin AY, Dzuban AV, Shestov VI, Gudkova YI, Brel VK, Tomilova LG, Zefirova NS. Peripheral functionalisation of a stable phthalocyanine J-type dimer to control the aggregation behaviour and NLO properties: UV-Vis, fluorescence, DFT, TDHF and thermal study. *RSC Adv* 2015;5(11):8239-47.
- [11] Rothmund S, Teasdale I. Preparation of polyphosphazenes: a tutorial review. *Chem Soc Rev* 2016;45(19):5200-15.
- [12] Allcock HR. Recent advances in phosphazene (phosphonitric) chemistry. *Chem Rev* 1972;72(4):315-56.

- [13] Craven M, Xiao D, Kunstmann-Olsen C, Kozhevnikova EF, Blanc F, Steiner A, Kozhevnikov IV. Oxidative desulfurization of diesel fuel catalyzed by polyoxometalate immobilized on phosphazene-functionalized silica. *Appl Catal B Environ* 2018;231:82–91.
- [14] Çoşut B, Yeşilot S, Durmuş M, Kılıç A. Synthesis and fluorescence properties of hexameric and octameric subphthalocyanines based cyclic phosphazenes. *Dyes Pigments* 2013;98(3):442–9.
- [15] Durmuş M, Yeşilot S, Çoşut B, Gürek AG, Kılıç A, Ahsen V. Comparison of photophysical properties of hexaphenoxycyclotriphosphazanyl-substituted metal-free, mono- and bis-lutetium phthalocyanines. *Synth Met* 2010;160(5):436–44.
- [16] Çoşut B, Yeşilot S, Durmuş M, Kılıç A, Ahsen V. Synthesis and properties of axially-phenoxycyclotriphosphazanyl substituted silicon phthalocyanine. *Polyhedron* 2010;29(2):675–82.
- [17] Allcock HR, Neenan TX. Synthesis of polyphosphazenes bearing covalently linked copper phthalocyanine units. *Macromolecules* 1986;19(6):1495–501.
- [18] Tolbin AY, Pushkarev Victor E, Tomilova LG, Zefirov NS. Selective synthesis of clamshell-type binuclear phthalocyanines. *Mendeleev Commun* 2009;19:78–80.
- [19] Schmidt MW, Baldrige KK, Boatz JA, Elbert ST, Gordon MS, Jensen JH, Koseki S, Matsunaga N, Nguyen KA, Su S, Windus TL, Dupuis M, Montgomery JA. General atomic and molecular electronic structure system. *J Comput Chem* 1993;14(11):1347–63.
- [20] Tolbin AY. The control system of the quantum-chemical calculations – EasyQuanto, Certificate of state registration of computer program No 2015619026 (RU). 2015.
- [21] Korostei YS, Tolbin AY, Dzuban AV, Pushkarev VE, Sedova MV, Maklakov SS, Tomilova LG. Monomeric aluminum complex based on A3B-type mono-hydroxy-functionalized phthalocyanine and its stable supramolecular J-type dimer: selective synthesis and physicochemical properties. *Dyes Pigments* 2018;149:201–11.
- [22] Kobayashi N, Nakajima S-i, Ogata H, Fukuda T. Synthesis, spectroscopy, and electrochemistry of tetra-tert-butylated tetraazaporphyrins, phthalocyanines, naphthalocyanines, and anthracocyanines, together with molecular orbital calculations. *Chem Eur J* 2004;10(24):6294–312.
- [23] Ortí E, Brédas JL, Clarisse C. Electronic structure of phthalocyanines: theoretical investigation of the optical properties of phthalocyanine monomers, dimers, and crystals. *J Chem Phys* 1990;92(2):1228–35.
- [24] Stuzhin PA, Bauer EM, Ercolani C. Tetrakis(thiadiazole)porphyrazines. 1. Syntheses and properties of tetrakis(thiadiazole)porphyrazine and its magnesium and copper derivatives. *Inorg Chem* 1998;37(7):1533–9.
- [25] Nemykin, V.N. and E.A. Lukyanets, 11 the key role of peripheral substituents in the chemistry of phthalocyanines, in *Handbook of porphyrin science*. p. 1-323.
- [26] Tolbin AY, Pushkarev VE, Shulishov EV, Tomilova LG. Directed synthesis of bi- and polynuclear clamshell-type phthalocyanines and their physico-chemical investigations. *J Porphyr Phthalocyanines* 2012;16(04):341–50.
- [27] Kodikara MS, Stranger R, Humphrey MG. Computational studies of the nonlinear optical properties of organometallic complexes. *Coord Chem Rev* 2018;375:389–409.
- [28] Karna SP, Dupuis M. Frequency dependent nonlinear optical properties of molecules: formulation and implementation in the HONDO program. *J Comput Chem* 1991;12(4):487–504.
- [29] Karakas A, Karakaya M, Taser M, Ceylan Y, Gozutok A, Arof AK, El Kouari Y, Sahraoui B. Computational studies on linear, second and third-order nonlinear optical properties of novel styrylquinolinium dyes. *Chem Phys Lett* 2016;648:47–52.